Guided-wave-coupled nitrogen vacancies in nanodiamond-doped photonic-crystal fibers

I. V. Fedotov, N. A. Safronov, Yu. A. Shandarov, A. A. Lanin, A. B. Fedotov et al.

Citation: Appl. Phys. Lett. **101**, 031106 (2012); doi: 10.1063/1.4731762
View online: http://dx.doi.org/10.1063/1.4731762
View Table of Contents: http://apl.aip.org/resource/1/APPLAB/v101/i3
Published by the American Institute of Physics.

Guided-wave-coupled nitrogen vacancies in nanodiamond-doped photonic-crystal fibers

I. V. Fedotov,[1] N. A. Safronov,[1] Yu. A. Shandarov,[1] A. A. Lanin,[1] A. B. Fedotov,[1] S. Ya. Kilin,[2] K. Sakoda,[3] M. O. Scully,[4,5] and A. M. Zheltikov[1,4]
[1]*Physics Department, Russian Quantum Center, International Laser Center, M.V. Lomonosov Moscow State University, Moscow 119992, Russia*
[2]*B.I. Stepanov Institute of Physics, National Academy of Sciences of Belarus, Minsk, Belarus*
[3]*National Institute for Materials Science, University of Tsukuba, 1-1 Namiki, Tsukuba 305-0044, Japan*
[4]*Department of Physics and Astronomy, Texas A&M University, College Station, Texas 77843, USA*
[5]*Department of Mechanical and Aerospace Engineering, Princeton University, Princeton, New Jersey 08544-5263, USA*

(Received 8 May 2012; accepted 1 June 2012; published online 17 July 2012)

Zero-phonon-line (ZPL) emission of nitrogen vacancies (NVs) is coupled to the guided modes of solid- and hollow-core nanodiamond-doped photonic-crystal fibers (PCFs). Both types of PCFs are tailored toward enhancing ZPL emission coupling to the fiber modes. In solid-core PCFs, this involves enhancing the evanescent field of the waveguide modes supported by an ultrasmall fiber core. In hollow-core PCFs, the NV emission spectrum is matched with the transmission band of the fiber, controlled by the photonic bands of the fiber cladding. © *2012 American Institute of Physics*. [http://dx.doi.org/10.1063/1.4731762]

The unique photophysics of nitrogen vacancies (NVs) in diamond is at the heart of rapidly growing diamond photonics, giving a powerful momentum to quantum information technologies,[1–4] bioimaging,[4,5] and nanoscale magnetic sensing.[6,7] The NV centers in diamond offer much promise for the creation of robust and reliable single-photon sources (see, e.g., Ref. 4 for a review), opening new horizons in quantum computations, quantum communications, and single-photon spectroscopy. The low photon outcoupling efficiency typical of NV centers in a bulk crystal and the necessity to connect NV centers into large-scale quantum information networks and distributed quantum computers call for the strategies that would allow NV centers to be coupled to optical waveguides. Several attractive and elegant solutions to this problem have been recently demonstrated, including fabrication of NV-center-embedded diamond nanowires,[8] placing diamond nanoparticles on a facet of a photonic-crystal fiber (PCF),[9] coupling NV diamond centers to a semiconductor waveguide,[10] and doping solid-core PCFs with NV diamond nanoparticles.[11]

Here, we report a direct coupling of the zero-phonon-line (ZPL) NV emission to the guided modes of solid- and hollow-core nanodiamond-doped PCFs. We demonstrate that both types of PCFs can be tailored toward enhancing ZPL emission coupling to the fiber modes using the evanescent field of waveguide modes in ultrasmall-silica-core PCFs and air-core-guided modes in hollow PCFs. Both PCF designs are shown to facilitate the detection of ZPL photons from low densities of diamond NV centers against the Raman background from the fiber.

Two types of photonic-crystal fibers, fabricated by means of standard PCF technologies,[12] were used in our experiments. Fiber of the first type (Fig. 1(a)) were designed in such a way as to provide efficient optical interrogation of NV centers in diamond nanoparticles by the evanescent field of fiber modes guided along the fiber core (Fig. 2(a)). To this end, PCFs with a core diameter on the order of 1 μm were chosen. In fibers of this class, a significant fraction of radiation power of the fundamental mode is guided as the evanescent field outside the fiber core. Moreover, the ratio of radiation energy localized in the fiber core to the energy of radiation guided in the evanescent field outside the fiber core can be controlled by tailoring the fiber structure.[13] The second type of fibers used in our experiments included hollow-core PCFs (Fig. 1(b)) with a core diameter of 15 μm. Diamond nanoparticles with NV centers were deposited on the walls of the fiber core (Fig. 2(b)) and were interrogated by air-guided modes of the hollow PCF within the transmission band of the fiber, controlled by the photonic bands of the two-dimensionally periodic fiber cladding.

In our experiments, the PCFs were infiltrated[11,14] with a syringe-pressurized fluid (water or ethanol) containing NV-diamond nanoparticles with a mean diameter of 300 nm. The NV centers that impregnate the fiber as a result of this procedure fill the air holes in the fiber structure along the entire fiber length. The liquid carrying the diamond nanoparticles was then dried out, with the NV-center nanodiamond left deposited on the walls of the air holes. The 532-nm, 100-mW second-harmonic output of a diode-pumped continuous-wave Nd:YAG laser was used as a source of optical pump (Fig. 3). The laser output was coupled into the PCF filled with NV-diamond nanoparticles using high-NA objectives. The photoluminescent response of the NV centers inside the fiber, detected in either forward or backward direction, was separated from the pump with a notch filter and a set of color-glass filters and was analyzed with a standard spectrometer (Fig. 3).

In the PCF of the first type (Fig. 1(a)), 532-nm pump radiation guided along a small silica core of the fiber provides excitation of the NV diamond centers with its evanescent field (Fig. 2(a)). The fiber core diameter for this type of nanodiamond-doped waveguide structure is chosen as a

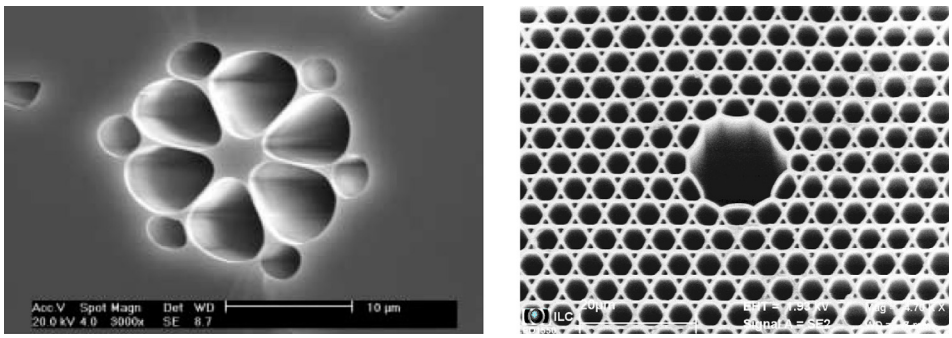

FIG. 1. SEM images of photonic-crystal fibers: (a) an ultrasmall-core PCF, (b) hollow-core PCF.

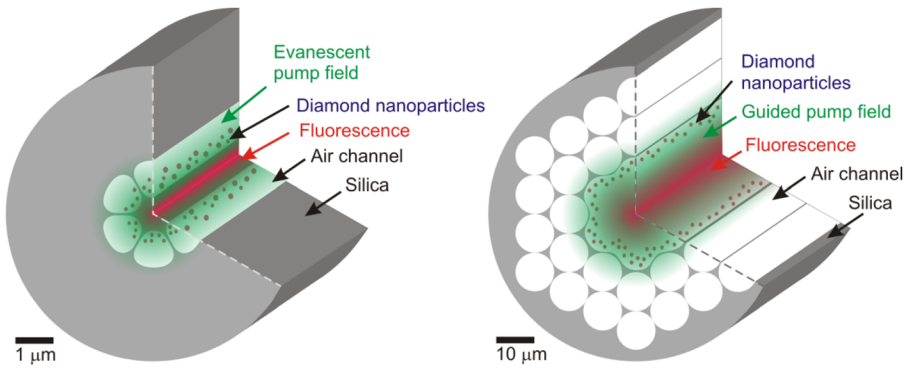

FIG. 2. Coupling nitrogen vacancies to waveguide modes of a nanodiamond-doped solid-core (a) and hollow-core (b) photonic crystal fiber.

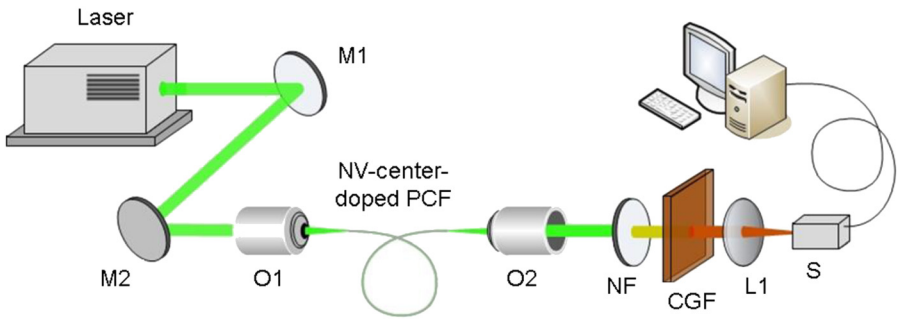

FIG. 3. Diagram of the experimental setup: M1, M2, mirrors; O1, O2, objectives; NF, notch filter; CGF, color-glass filter; L1, lens; S, spectrometer.

compromise between the energy of the evanescent field, which is controlled by the fraction of the mode energy carried by the evanescent-field tails outside the fiber core, and the waveguide and beam-incoupling losses, which tend to dramatically increase with a decrease in the fiber core diameter. Specifically, for the PCF shown in Fig. 1(a) with a core diameter $d \approx 1.2\,\mu$m, according to our finite-element analysis, approximately 18% of radiation power of the fundamental mode at a wavelength of 532 nm is localized in the air holes, enabling efficient optical interrogation of diamond nanoparticles deposited on the silica walls of the air holes in the microstructured fiber cladding. The waveguide loss for this type of PCF at the pump wavelength was estimated as 100 dB/km. The maximum beam-incoupling efficiency achieved in our experiments with this PCF was 50%.

For PCFs doped with relatively high densities of NV centers (higher than 10^4 per 1 cm of PCF), the spectra of the photoluminescent response collected from the output end of the NV-center-doped PCF (curve 1 in Fig. 4(a)) are almost identical to the spectra measured from an ensemble of nanoparticles in a cell or on a substrate (curve 3 in Fig. 4(b)). These spectra display well-resolved peaks centered at 575 and 637 nm, corresponding to the ZPLs of the neutral (NV^0) and negatively charged (NV^-) NV centers in diamond. The efficiency of conversion of 50-mW, 532-nm pump to the photoluminescent response of NV centers in this regime for a PCF with a core diameter of 1.2 μm is estimated as 10^{-5} for a 10-cm piece of NV-center-doped PCF.

At low densities of NV centers in the PCF, however, the photoluminescence spectra collected from the PCF become distorted by the Raman signal (curve 1 in Fig. 4(b)), which is inevitably generated by the optical pump in silica inside the fiber (curve 2 in Figs. 4(a) and 4(b)), making it one of the key issues of fiber components intended for the delivery of low-intensity optical signals. In the PCF format, the level of the Raman background can be radically reduced by decreasing the content of silica in the fiber, i.e., by increasing the air-filling fraction in the PCF. For a PCF with the cross-section structure as shown Fig. 1(a), the high air-filling fraction of the cladding allows the 637-nm ZPL line of NV^- centers to be reliably detected against the Raman background (curve 1 in Fig. 4(b)) for the density of NV centers in the fiber as low as 10^3 per 1 cm of fiber. Since both the Raman signal from the fiber and the photoluminescence from NV centers scale linearly with the pump power, the ratio of the intensity of the ZPL line from NV centers to the Raman

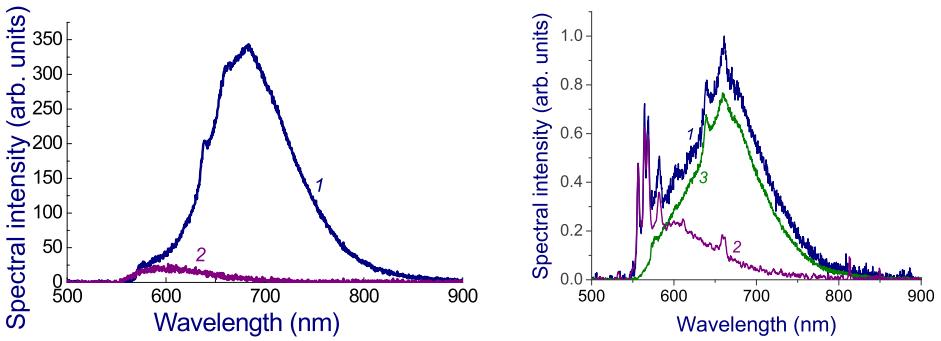

FIG. 4. Spectra of NV center emission from a nanodiamond-doped ultrasmall-core PCF (1), the Raman background from the same fiber (2), and NV center emission from a glass substrate (3). The density of NV centers is 5×10^4 (a) and 10^3 (b) per 1 cm of fiber.

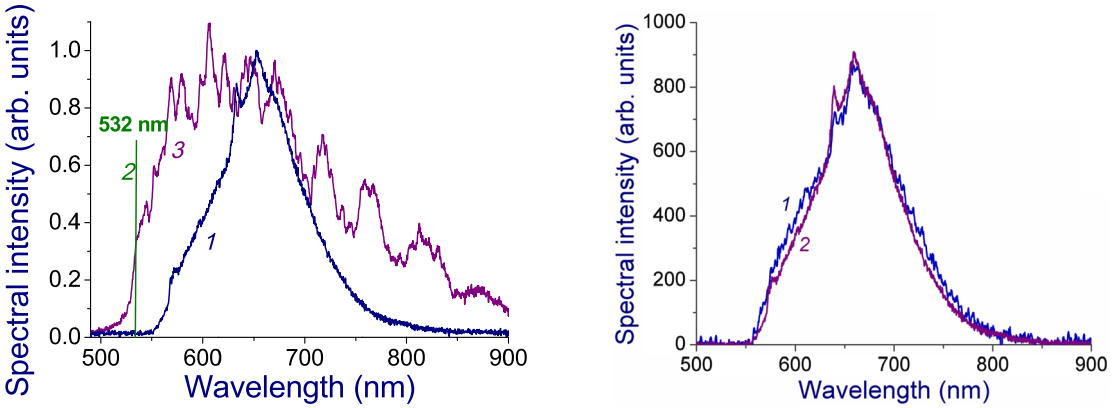

FIG. 5. (a) Spectra of NV center emission from a nanodiamond-doped hollow-core PCF (1), 532-nm excitation radiation (2), and fiber transmission (3). (b) Spectra of NV center emission from nanodiamond-doped hollow-core PCF (1) and from a glass substrate (2). The density of NV centers is 10^4 per 1 cm of fiber.

background is expected to remain unchanged for the pump power level necessary for the single-photon regime of the PCF-format NV light source.

The ZPL-signal-to-Raman-background ratio for NV-center-doped fibers can be further improved with a hollow-core PCF fiber design. In fibers of this type (Fig. 1(b)), even though the refractive index of the fiber core is lower than the refractive index of the cladding, radiation can be confined to the fiber core due to the high reflectivity of the two-dimensionally periodic cladding within the bands of low density of photonic states (e.g., photonic band gaps) of the fiber cladding.[12] For efficient excitation of NV centers and enhanced coupling of the ZPL photoluminescent response of these centers to the fiber modes, hollow PCFs should be designed in such a way as to support the air guiding for both pump and ZPL photoluminescence of NV centers with a maximum possible overlap of the radial profile of the pump field with diamond nanoparticles deposited on the walls of the hollow fiber core (Fig. 2(b)). These somewhat conflicting requirements are fulfilled with a hollow PCF structure used in our experiments (Fig. 1(b)). This fiber supports air-guided modes of the pump field, whose carrier frequency is, however, off the center of the transmission band of the PCF (cf. curves 2 and 3 in Fig. 5(a)), providing for the spatial overlap between the pump field and the diamond nanoparticles. The photoluminescence spectrum of the NV centers is, on the other hand, matched with the transmission spectrum of the fiber (cf. curves 1 and 3 in Fig. 5(a)), providing efficient coupling of the photoluminescence response from the NV centers to the air-guided modes of the PCF, thus allowing fiber-format filtering of this signal from the Raman signal generated in the fiber cladding. As can be seen from Fig. 5(b), this fiber design provides high ZPL-signal-to-Raman-background ratios even at low levels of nanodiamond doping. For a density of NV centers of 10^4 per 1 cm of PCF, the contribution of the Raman background to the overall output signal is below 1%, allowing a reliable detection of the ZPL response from NV centers.

To summarize, we have demonstrated a direct coupling of ZPL emission from nitrogen vacancies of diamond to the guided modes of solid- and hollow-core nanodiamond-doped PCFs. Both types of PCFs have been tailored toward enhancing ZPL emission coupling to the fiber modes using the evanescent field of waveguide modes in ultrasmall-silica-core PCFs and air-core-guided modes in hollow PCFs. Both PCF designs have been shown to facilitate the detection of ZPL photons from low densities of diamond NV centers against the Raman background from the fiber.

This work was supported in part by the Russian Foundation for Basic Research (projects 11-02-92012, 10-02-91226, and 11-02-92118), the Welch Foundation (Grant No. A-1801), and the Seventh European Framework Programme (CROSS TRAP 244068 project).

[1]J. Wrachtrup, S. Ya. Kilin, and A. P. Nizovtsev, Opt. Spectrosc. **91**, 429 (2001).
[2]T. Gaebel, M. Domhan, I. Popa, C. Wittmann, P. Neumann, F. Jelezko, J. R. Rabeau, N. Stravrias, A. D. Greentree, S. Prawer, J. Meijer, J. Twamley, P. R. Hemmer, and J. Wrachtrup, Nat. Phys. **2**, 408 (2006).
[3]M. V. G. Dutt, L. Childress, L. Jiang, E. Togan, J. Maze, F. Jelezko, A. S. Zibrov, P. R. Hemmer, and M. D. Lukin, Science **316**, 1312 (2007).

[4]I. Aharonovich, A. D. Greentree, and S. Prawer, Nat. Photonics **5**, 397 (2011).
[5]L. P. McGuinness, Y. Yan, A. Stacey, D. A. Simpson, L. T. Hall, D. Maclaurin, S. Prawer, P. Mulvaney, J. Wrachtrup, F. Caruso, R. E. Scholten, and L. C. L. Hollenberg, Nat. Nanotechnol. **6**, 358 (2011).
[6]J. M. Taylor, P. Cappellaro, L. Childress, L. Jiang, D. Budker, P. R. Hemmer, A. Yacoby, R. Walsworth, and M. D. Lukin, Nat. Phys. **4**, 810 (2008).
[7]G. Balasubramanian, I. Y. Chan, R. Kolesov, M. Al-Hmoud, J. Tisler, C. Shin, C. Kim, A. Wojcik, P. R. Hemmer, A. Krueger, T. Hanke, A. Leitenstorfer, R. Bratschitsch, F. Jelezko, and J. Wrachtrup, Nature **455**, 648 (2008).
[8]T. M. Babinec, B. J. M. Hausmann, M. Khan, Y. Zhang, J. R. Maze, P. R. Hemmer, and M. Lončar, Nat. Nanotechnol. **5**, 195 (2010).
[9]T. Schröder, A. W. Schell, G. Kewes, T. Aichele, and O. Benson, Nano Lett. **11**, 198 (2011).
[10]K.-M. C. Fu, C. Santori, P. E. Barclay, I. Aharonovich, S. Prawer, N. Meyer, A. M. Holm, and R. G. Beausoleil, Appl. Phys. Lett. **93**, 234107 (2008).
[11]I. V. Fedotov, N. A. Safronov, Yu. A. Shandarov, A. Yu. Tashchilina, A. B. Fedotov, A. P. Nizovtsev, D. I. Pustakhod, V. N. Chizevski, T. V. Matveeva, K. Sakoda, S. Ya. Kilin, and A. M. Zheltikov, Laser Phys. Lett. **9**, 151 (2012).
[12]P. St. J. Russell, Science **299**, 358 (2003).
[13]A. Zheltikov, J. Opt. Soc. Am. B **22**, 1100 (2005).
[14]A. A. Voronin, V. P. Mitrokhin, A. A. Ivanov, A. B. Fedotov, D. A. Sidorov-Biryukov, V. I. Beloglazov, M. V. Alfimov, H. Ludvigsen, and A. M. Zheltikov, Laser Phys. Lett. **7**, 46 (2010).